Inorg. Chem. **2004**, *43*, 8310–8317

The Zinspy Family of Fluorescent Zinc Sensors: Syntheses and Spectroscopic Investigations

Elizabeth M. Nolan and Stephen J. Lippard*

Department of Chemistry, Massachusetts Institute of Technology, Cambridge, Massachusetts 02139

Received September 1, 2004

Four fluorescent sensors designed for Zn(II) detection that contain a fluorescein reporting group and a pyridylamine-thioether derivatized ligand moiety were prepared and their photophysical properties characterized. These "Zinspy" sensors are water soluble and generally display ~1.4- to ~4.5-fold fluorescence enhancement upon Zn(II) coordination, depending upon fluorescein halogenation and the number and nature of the zinc-binding appendages. The Zinspy sensors exhibit improved selectivity for zinc compared to the di-(2-picolyl)amine-based Zinpyr family.

Introduction

The creation of new tools and approaches for optical imaging in biology is an important goal, and investigations focused on these objectives will ultimately increase our understanding of many biological phenomena. Zinc is an essential nutrient required for normal growth and development[1] and for key cellular processes such as DNA repair[2,3] and apoptosis.[4] Zinc concentrations are tightly regulated under normal physiological conditions.[1,5] Failure to maintain zinc homeostasis has been implicated in a number of pathologies including diabetes[6] and Alzheimer's disease.[7−9] Although most physiological zinc is tightly bound in metalloproteins,[1,10] histochemically observable zinc exists in several tissues including the brain.[11−15] In the glutamatergic neurons of the hippocampus, the center of learning and memory in the brain, concentrations of loosely bound or "free" zinc may reach near-millimolar concentrations.[11] These zinc pools contain ~5% of total brain zinc, the physiological and pathological significance of which remains unclear.[12,16,17] Recent observations suggest that free zinc plays a number of beneficial and deleterious roles in neurobiology.[12,18−22] Our understanding of these phenomena has been hampered, in part, because of a lack of versatile zinc imaging tools.[23] The development and application of new zinc chemosensors for neurobiological investigations should ultimately help elucidate the significance of zinc in neurotransmission and memory formation, and in the pathogenesis of various neurological disorders.[24−34]

* To whom correspondence should be addressed. E-mail: lippard@mit.edu.

(1) Vallee, B. L.; Falchuk, K. H. *Physiol. Rev.* **1993**, *73*, 79−118.
(2) Ho, E.; Ames, B. N. *Prod. Natl. Acad. Sci. U.S.A.* **2002**, *99*, 16770−16775.
(3) Daiyasu, H.; Osaka, K.; Ishino, Y.; Toh, H. *FEBS Lett.* **2001**, *503*, 1−6.
(4) Troung-Tran, A. Q.; Carter, J.; Ruffin, R. E.; Zalewski, P. D. *Biometals* **2001**, *14*, 315−330.
(5) Takeda, A. *Biometals* **2001**, *14*, 343−351.
(6) Chausmer, A. B. *J. Am. Coll. Nutr.* **1998**, *17*, 109−115.
(7) Bush, A. I. *Trends Neurosci.* **2003**, *26*, 207−214.
(8) Suh, S. W.; Jensen, K. B.; Jensen, M. S.; Silva, D. S.; Kesslak, P. J.; Danscher, G.; Frederickson, C. J. *Brain Res.* **2000**, *852*, 274−278.
(9) Bush, A. I. *Alzheimer Dis. Assoc. Disord.* **2003**, *17*, 147−150.
(10) Lippard, S. J.; Berg, J. M. *Principles of Bioinorganc Chemistry*, 1st ed.; University Science Books: Mill Valley, CA, 1994.
(11) Frederickson, C. J. *Int. Rev. Neurobiol.* **1989**, *31*, 145−238.
(12) Frederickson, C. J.; Bush, A. I. *Biometals* **2001**, *14*, 353−366.
(13) Qian, W.-J.; Gee, K. R.; Kennedy, R. T. *Anal. Chem.* **2003**, *75*, 3468−3475.
(14) Gee, K. R.; Zhou, Z.-L.; Qian, W.-J.; Kennedy, R. *J. Am. Chem. Soc.* **2002**, *124*, 776−778.
(15) Zalewski, P. D.; Millard, S. H.; Forbes, I. J.; Kapaniris, O.; Slavotinek, A.; Betts, W. H.; Ward, A. D.; Lincoln, S. F.; Mahadevan, I. *J. Histochem. Cytochem.* **1994**, *42*, 877−884.
(16) Kay, A. R. *J. Neurosci.* **2003**, *23*, 6847−6855.
(17) Frederickson, C. J.; Maret, W.; Cuajungco, M. P. *Neuroscientist* **2004**, *10*, 18−25.
(18) Cuajungo, M. P.; Lees, G. J. *Neurobiol. Dis.* **1997**, *4*, 137−169.
(19) Choi, D. W.; Koh, J. Y. *Annu. Rev. Neurosci.* **1998**, *21*, 347−375.
(20) Bush, A. I. *Curr. Opin. Chem. Biol.* **2000**, *4*, 184−191.
(21) Li, Y.; Hough, C. J.; Frederickson, C. J.; Sarvey, J. M. *J. Neurosci.* **2001**, *21*, 8015−8025.
(22) Li, Y. V.; Hough, C. J.; Sarvey, J. M. *Science STKE* **2003**, pe 19.
(23) Frederickson, C. J. *Science STKE* **2003**, pe 18.
(24) Henary, M. M.; Fahrni, C. J. *J. Phys. Chem. A* **2002**, *106*, 5210−5220.
(25) Henary, M. M.; Wu, Y.; Fahrni, C. J. *Chem. Eur. J.* **2004**, *10*, 3015−3025.
(26) Frederickson, C. J.; Kasarskis, E. J.; Ringo, D.; Frederickson, R. E. *J. Neurosci. Methods* **1987**, *20*, 91−103.
(27) Taki, M.; Wolford, J. L.; O'Halloran, T. V. *J. Am. Chem. Soc.* **2004**, *126*, 712−713.
(28) Maruyama, S.; Kikuchi, K.; Hirano, T.; Urano, Y.; Nagano, T. *J. Am. Chem. Soc.* **2002**, *124*, 10650−10651.

10.1021/ic048778z CCC: $27.50
Published on Web 12/02/2004

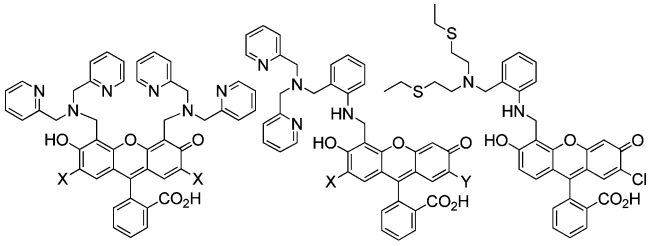

Figure 1. Representative members of the ZP family of zinc sensors and mercury sensor MS1.

To address the need for fluorescent probes designed to detect zinc in biological samples, our laboratory has synthesized, characterized, and utilized the Zinpyr (ZP) family of zinc sensors.[35−40] These water-soluble, fluorescein-based probes, several of which are depicted in Figure 1, display a 1.6- to 11-fold fluorescence enhancement upon zinc coordination depending upon the nature of the fluorescein platform and its zinc-binding appendages. All ZP chemosensors contain either one or two di(2-picolyl)amine (DPA) derived ligands and exhibit excellent selectivity for Zn(II) over Mn(II) and the biologically abundant cations Na(I), K(I), Mg(II), and Ca(II).

The high affinity of DPA for all divalent first-row transition metal ions, such as Fe(II) and Cu(II), is one disadvantage of the ZP family of zinc sensors. Metal-ion selectivity studies of ZP probes reveal that Co(II), Fe(II), Ni(II), and Cu(II) compromise Zn(II)-induced fluorescence turn-on. With the aim of increasing the selectivity of our sensors for zinc over other first-row transition metal ions while maintaining fluorescence enhancement upon zinc coordination, we are currently investigating new ligand frameworks for use in zinc sensing, a number of which include both nitrogen and sulfur donors. Two inspirations for assessing the utility of sulfur donors in zinc sensing come from the ubiquity of Zn−S linkages in biology[10] and from our successful use of a thioether-derivatized fluorescein-based sensor, shown in Figure 1, for the detection of mercuric ion, a congener of Zn(II), in aqueous media.[41]

In the present article, we introduce the Zinspy (ZS) family of zinc sensors, which contain pyridyl−amine−thioether ligands. Like the ZP family, the ZS probes are based on a fluorescein platform, display water solubility, and generally exhibit a fluorescence turn-on following zinc coordination.

Experimental Section

Reagents. Ethyl acetate was dried over 3 Å molecular sieves. Anhydrous methanol and anhydrous 1,2-dichloroethane (DCE) were purchased from Aldrich and used as received. Acetonitrile was saturated with Ar and dried by passing through Al_2O_3 columns. The asymmetrically derivatized fluoresceins, 7′-chloro-4′-fluoresceincarboxaldehyde, **4**, and 7′-chloro-4′-bromomethylfluorescein di-*tert*-butylsilyl ether, **8**, were synthesized as described elsewhere.[37,39] 2′,7′-Difluorofluorescein was purchased from Molecular Probes, 2-(ethylthio)ethylamine was obtained from Alfa Aesar, and all other chemicals were purchased from Aldrich. With the exception of 2′,7′-dichlorofluorescein, which was recrystallized from EtOH, all reagents were used as received.

Materials and Methods. Merck F254 silica gel-60 plates or octadecyl-functionalized silica gel (reverse phase, RP18) plates were used for analytical thin-layer chromatography (TLC). Preparative TLC was performed by using EM Science RP18 plates of 1 mm thickness. NMR spectra were obtained by using either a Varian 300 MHz or a Varian 500 MHz spectrometer operating at ambient probe temperature, 283 K. Internal probe standards were used for ^{1}H and ^{13}C NMR, and an external $CFCl_3$ reference was used for ^{19}F NMR spectroscopy. An Avatar 360 FTIR instrument was used to collect IR spectra. Low resolution mass spectra were obtained by using an Agilent 1100 Series LC/MSD system. High-resolution mass spectrometry was performed by staff at the MIT Department of Chemistry Instrumentation Facility.

(2-Ethylsulfanylethyl)pyridin-2-ylmethylamine (1). Portions (1.0 g, 9.5 mmol) of 2-(ethylthio)ethylamine and 2-pyridinecarboxaldehyde (1.0 g, 9.4 mmol) were combined in 30 mL of dry MeOH to yield a light yellow solution that was stirred at room temperature. The solution turned brown, and after 18 h, $NaB(OAc)_3H$ (2.4 g, 11 mmol) was added in two equal portions over 30 min. The mixture was stirred overnight at room temperature, and the solvent was removed under reduced pressure to yield a brown oil. The oil was dissolved in CH_2Cl_2 (60 mL) and washed with saturated $NaHCO_3$ (3 × 60 mL) and water (1 × 60 mL). The organic portion was dried over $MgSO_4$, and the solvent was removed in vacuo to yield a brown oil. Flash chromatography on silica gel (10:1 $CHCl_3$/MeOH) afforded the purified product as a brown oil (1.01 g, 54%). TLC R_f = 0.46 (silica, 10:1 $CHCl_3$/MeOH). ^{1}H NMR ($CDCl_3$, 300 MHz) δ 1.16 (3H, t), 2.44 (2H, q), 2.63 (2H, m), 2.78 (2H, t), 3.86 (2H, s), 7.07 (1H, m), 7.24 (1H, d), 7.55 (1H, t), 8.47 (1H, m). ^{13}C NMR ($CDCl_3$, 125 MHz) δ 14.75, 25.61, 31.72, 48.10, 54.72, 121.86, 122.09, 136.37, 149.19, 159.50. FTIR (NaCl disk, cm^{-1}) 3302 (m, br), 3050 (w), 3008 (w), 2963 (s), 2923 (s), 2870 (s), 2828 (s), 1711 (w), 1675 (w), 1590 (s), 1569 (s), 1473 (s), 1454 (s), 1433 (s), 1374 (m), 1356 (m), 1296 (w), 1264 (m), 1125 (w), 1048 (m), 994 (m), 973 (m), 844 (m), 756 (s), 628 (m), 609 (m). HRMS (ESI) Calcd MH$^+$, 197.1107. Found, 197.1114.

(2-Ethylsulfanylethyl)(2-nitrobenzyl)pyridin-2-ylmethylamine (2). To 25 mL of MeCN were added **1** (500 mg, 3.06 mmol), 2-nitrobenzylbromide (662 mg, 3.06 mmol), K_2CO_3 (600 mg, 4.34 mmol), and activated 3 Å molecular sieves. The reaction was stirred

(29) Hirano, T.; Kikuchi, K.; Urano, Y.; Nagano, T. *J. Am. Chem. Soc.* **2002**, *124*, 6555−6562.
(30) Woodroofe, C. C.; Lippard, S. J. *J. Am. Chem. Soc.* **2003**, *125*, 11458−11459.
(31) Chang, C. J.; Jaworski, J.; Nolan, E. M.; Sheng, M.; Lippard, S. J. *Proc. Natl. Acad. Sci. U.S.A.* **2003**, *101*, 1129−1134.
(32) Sensi, S. L.; Ton-That, D.; Weiss, J. H.; Rothe, A.; Gee, K. R. *Cell Calcium* **2003**, *34*, 281−284.
(33) Jiang, P.; Guo, Z. *Coord. Chem. Rev.* **2004**, *248*, 205−229.
(34) Kikuchi, K.; Komatsu, K.; Nagano, T. *Curr. Opin. Chem. Biol.* **2004**, *8*, 182−191.
(35) Walkup, G. K.; Burdette, S. C.; Lippard, S. J.; Tsien, R. Y. *J. Am. Chem. Soc.* **2000**, *122*, 5644−5645.
(36) Burdette, S. C.; Walkup, G. K.; Spingler, B.; Tsien, R. Y.; Lippard, S. J. *J. Am. Chem. Soc.* **2001**, *123*, 7831−7841.
(37) Burdette, S. C.; Frederickson, C. J.; Bu, W.; Lippard, S. J. *J. Am. Chem. Soc.* **2003**, *125*, 1778−1787.
(38) Chang, C. J.; Nolan, E. M.; Jaworski, J.; Burdette, S. C.; Sheng, M.; Lippard, S. J. *Chem. Biol.* **2004**, *11*, 203-210.
(39) Nolan, E. M.; Burdette, S. C.; Harvey, J. H.; Hilderbrand, S. A.; Lippard, S. J. *Inorg. Chem.* **2004**, *43*, 2624−2635.
(40) Chang, C. J.; Nolan, E. M.; Jaworski, J.; Okamoto, K.-I.; Hayashi, Y.; Sheng, M.; Lippard, S. J. *Inorg. Chem.* **2004**, *43*, 6774−6779.
(41) Nolan, E. M.; Lippard, S. J. *J. Am. Chem. Soc.* **2003**, *125*, 14270−14271.

vigorously at room temperature for 24 h and filtered through Celite, and the solvent was removed in vacuo to yield a brown oil. The crude material was flushed through a plug of silica gel (4:1 hexanes/EtOAc) to yield the pure product as a yellow oil (743 mg, 73%). TLC $R_f = 0.35$ (silica, 2:1 hexanes/EtOAc). ^{1}H NMR ($CDCl_3$, 300 MHz) δ 1.15 (3H, m), 2.39 (2H, q), 2.56−2.71 (4H, m), 3.75 (2H, s), 4.01 (2H, s), 7.11 (1H, m), 7.33−7.49 (2H, m), 7.51 (1H, td), 7.61 (1H, td), 7.72 (1H, d), 7.78 (1H, dd), 8.46 (1H, m). ^{13}C NMR ($CDCl_3$, 125 MHz) δ 14.86, 26.07, 28.80, 54.26, 56.08, 60.46, 122.24, 123.08, 124.52, 128.14, 131.25, 132.63, 134.64, 136.66, 148.92, 149.93, 159.10. FTIR (NaCl disk, cm^{-1}) 3064 (w), 3008 (w), 2963 (m), 2926 (m), 2828 (m), 2721 (w), 1608 (m), 1589 (s), 1570 (m), 1528 (s), 1474 (m), 1434 (m), 1362 (s), 1302 (m), 1265 (m), 1147 (m), 1114 (m), 1089 (m), 1047 (m), 994 (m), 973 (m), 857 (m), 819 (w), 783 (m), 760 (s), 730 (s), 705 (w), 668 (m), 638 (w), 617 (w). HRMS (ESI) Calcd MH$^+$, 332.1427. Found, 332.1417.

2-{[(2-Ethylsulfanylethyl)pyridin-2-ylmethylamino]methyl}-phenylamine (3). Palladium black (606 mg) and 10 mL of MeOH were combined in a flask purged with Ar. A portion (308 mg, 0.929 mmol) of **2** was dissolved in 15 mL of MeOH and added to the reaction flask. The flask was purged with H_2, and the reaction was stirred vigorously under H_2 for 1.5 h. The mixture was filtered through Celite, and the solvent was removed under reduced pressure. Chromatography on Al_2O_3 with a solvent gradient (5:1 to 1:1 hexanes/EtOAc) yielded the product as a yellow-orange oil (191 mg, 68%). TLC $R_f = 0.45$ (Al_2O_3, 3:1 hexanes/EtOAc). ^{1}H NMR ($CDCl_3$, 300 MHz) δ 1.14 (3H, m), 2.35 (2H, m), 2.64−2.75 (2H, m), 3.66 (2H, s), 3.73 (2H, s), 4.80 (2H, br s), 6.60−6.67 (2H, m), 7.00−7.14 (3H, m), 7.30 (1H, d), 7.60 (1H, td), 8.50 (1H, dq). ^{13}C NMR ($CDCl_3$, 125 MHz) δ 14.76, 25.78, 28.99, 53.26, 58.18, 60.09, 115.53, 117.50, 122.10, 122.33, 123.52, 128.60, 130.94, 136.36, 146.99, 149.00, 159.23. FTIR (NaCl disk, cm^{-1}) 3423 (s), 3314 (s), 3208 (m), 3009 (m), 2962 (s), 2924 (s), 2869 (m), 2813 (s), 2717 (w), 1616 (s), 1590 (s), 1569 (m), 1495 (s), 1474 (m), 1460 (s), 1433 (s), 1373 (m), 1315 (m), 1288 (m), 1265 (m), 1148 (m), 1125 (m), 1104 (m), 1048 (m), 995 (m), 969 (m), 932 (w), 869 (w), 847 (w), 752 (s), 723 (w), 637 (w) 614 (w), 541 (w). HRMS (ESI) Calcd MH$^+$, 302.1685. Found, 302.1694.

2-{2-Chloro-5-[(2-{[(2-ethylsulfanylethyl)pyridin-2-ylmethylamino]methyl}phenylamino)methyl]-6-hydroxy-3-oxo-3,10-dihydroanthracen-9-yl}benzoic Acid (5, Zinspy-4, ZS4). Portions (53 mg, 0.192 mmol) of **3** and **4** (68 mg, 0.172 mmol) were combined in 3 mL of EtOAc and stirred overnight at room temperature. The intermediate Schiff base precipitated as a bright yellow solid. The reaction was cooled on ice and filtered, and the precipitate was washed with ∼3 mL of cold EtOAc and dried. The precipitate was dissolved in 5 mL of DCE, and $NaB(OAc)_3H$ (60 mg, 0.28 mmol) was added. The reaction was stirred at room temperature for 6 h, diluted with 5 mL of CH_2Cl_2, and washed with H_2O (3 × 10 mL). The organic layer was dried to yield a red-orange solid (71 mg, 60%, purity > 90% by NMR). A portion (∼32 mg) of the crude material was purified by preparative TLC on reverse phase silica gel (100% MeOH) to yield the product as a red-orange solid (18 mg, 56% recovered). TLC $R_f = 0.69$ (RP18 silica, MeOH); mp = 89−91 °C. ^{1}H NMR ($CDCl_3$, 300 MHz) δ 1.10 (3H, t), 2.30 (2H, q), 2.63−2.71 (4H, m), 3.75 (4H, m), 4.78 (2H, s), 6.54 (2H, m), 6.76−6.95 (5H, m), 7.07−7.27 (5H, m), 7.58−7.72 (2H, m), 8.05 (1H, d), 8.49 (1H, d). FTIR (KBr, cm^{-1}) 3436 (s), 2963 (w), 2924 (w), 2853 (w), 1761 (m), 1674 (s), 1625 (m), 1613 (m), 1514 (w), 1455 (m), 1422 (m), 1375 (w), 1261 (s), 1201 (s), 1178 (s), 1092 (s), 1022 (s), 871 (w), 800 (s), 757 (w), 720 (w), 702 (w). HRMS (ESI) Calcd MH$^+$, 680.1980. Found, 680.1962.

2-(2,7-Dichloro-4,5-bis-{[(2-ethylsulfanylethyl)pyridin-2-ylmethylamino]methyl}-6-hydroxy-3-oxo-3*H*-xanthen-9-yl)benzoic Acid (6, Zinspy-1, ZS1). Paraformaldehyde (12 mg, 0.41 mmol) and **1** (79 mg, 0.31 mmol) were combined in MeCN (6 mL) and refluxed for 1 h. A slurry of 2′,7′-dichlorofluorescein (50 mg, 0.13 mmol) in 1:1 MeCN/H_2O (6 mL) was added to the reaction, and the solution immediately turned pink-red. The reaction was refluxed for 24 h and cooled, and the solvents were removed under reduced pressure. Preparative TLC on reverse phase silica gel (100% MeOH) yielded the purified product as an orange-pink solid (69 mg, 67%). TLC $R_f = 0.44$ (RP18 silica, MeOH); mp = 79−80 °C. ^{1}H NMR (CD_3OD, 300 MHz) δ 1.14 (6H, t), 2.41 (4H, q), 2.79 (4H, t), 2.97 (4H, t), 4.07 (4H, s), 4.24 (4H, s), 6.61 (2H, s), 7.24 (1H, d), 7.34 (2H, t), 7.46 (2H, d), 7.71−7.80 (4H, m), 8.06 (1H, d), 8.55 (2H, d). ^{13}C NMR (DMF-d_7, 125 MHz) δ 14.66, 25.45, 28.13, 49.90, 53.50, 58.22, 82.81, 110.72, 112.09, 116.96, 123.20, 124.21, 124.46, 125.42, 127.05, 127.15, 130.90, 136.11, 137.63, 148.77, 149.17, 152.14, 156.58, 157.43, 168.77. FTIR (KBr, cm^{-1}) 3121 (w), 2967 (w), 2923 (w), 2851 (w), 1760 (s), 1625 (m), 1597 (m), 1572 (m), 1466 (s), 1434 (s), 1399 (s), 1283 (s), 1262 (m), 1211 (m), 1152 (w), 1095 (s), 1013 (m), 889 (w), 867 (m), 801 (w), 758 (m), 727 (w), 699 (m), 676 (w), 619 (w), 560 (w), 482 (w). LRMS (ESI) Calcd MH$^-$, 815.2. Found, 815.5.

2-(4,5-Bis-{[(2-ethylsulfanylethyl)pyridin-2-ylmethylamino]-methyl}-2,7-difluoro-6-hydroxy-3-oxo-3*H*-xanthen-9-yl)benzoic Acid (7, Zinspy-2, ZS2). Paraformaldehyde (13.1 mg, 0.452 mmol) and **1** (80.6 mg, 0.411 mmol) were combined in MeCN (6 mL) and refluxed for 1 h. A slurry of 2′,7′-difluorofluorescein (50.0 mg, 0.136 mmol) in 1:1 MeCN/H_2O (6 mL) was added to the reaction, and the solution immediately turned pink-red. The reaction was refluxed for 24 h and cooled, and the solvents were removed under reduced pressure. Preparative TLC on reverse phase silica gel (100% MeOH) yielded the purified product as an orange-pink solid (42 mg, 39%). TLC $R_f = 0.36$ (RP18 silica, MeOH); mp = 65−67 °C. ^{1}H NMR (CD_3OD, 300 MHz) δ 1.15 (6H, t), 2.43 (4H, q), 2.87 (4H, t), 3.17 (4H, t), 4.24 (4H, s), 4.42 (4H, s), 6.54 (2H, d), 7.22 (1H, d), 7.33 (2H, t), 7.47 (2H, d), 7.68−7.81 (4H, m), 8.09 (1H, d), 8.52 (2H, d). ^{13}C NMR (DMF-d_7, 125 MHz) δ 14.67, 25.47, 28.30, 49.65, 53.74, 58.35, 108.61, 112.58, 112.75, 113.38, 123.11, 124.07, 124.47, 125.43, 127.15, 130.72, 135.88, 137.64, 146.32, 147.48, 149.03, 149.40, 157.80, 168.78. ^{19}F NMR (300 MHz) δ 27.62. FTIR (KBr, cm^{-1}) 3392 (m, br), 2962 (m), 2923 (m), 2851 (m), 1760 (m), 1701 (w), 1647 (m), 1606 (m), 1570 (w), 1559 (w), 1476 (s), 1438 (s), 1394 (m), 1373 (s), 1289 (s), 1262 (m), 1204 (m), 1163 (m), 1098 (m), 1043 (m), 864 (w), 802 (w), 761 (m), 717 (w), 635 (w), 577 (w), 520 (w). LRMS (ESI) Calcd MH$^-$, 783.3. Found, 783.3.

2-(2-Chloro-5-{[(2-ethylsulfanylethyl)pyridin-2-ylmethylamino]methyl}-6-hydroxy-3-oxo-3*H*-xanthen-9-yl)benzoic Acid (9, Zinspy-3, ZS3). To 3 mL of MeCN were added 2′-chloro-5′-bromomethylfluorescein di-*tert*-butyldimethylsilyl ether (**8**, 100 mg, 0.146 mmol) and K_2CO_3 (100 mg, 0.724 mmol), and the solution was stirred. A portion (20 mg, 0.148 mmol) of **1** was dissolved in 2 mL of MeCN and added dropwise to the reaction mixture. The color changed from yellow-orange to pink, and the reaction was stirred overnight at room temperature. A pink precipitate formed, and the solution was filtered. TLC analysis on RP18 silica (100% MeOH) showed that both the filtrate and precipitate contained the desired product. Preparative TLC on RP18 silica (100% MeOH) afforded pure ZS3 as an orange solid (70 mg, 83%). TLC $R_f = 0.65$ (RP18 silica, MeOH); mp = 97−100 °C. ^{1}H NMR (CD_3OD, 300 MHz) δ 1.15 (3H, t), 2.42 (2H, q), 2.85 (2H, t), 3.01 (2H, t), 4.08 (2H, s), 4.28 (2H, s), 6.56 (1H, d), 6.67 (1H, d), 6.77 (1H, s),

Scheme 1

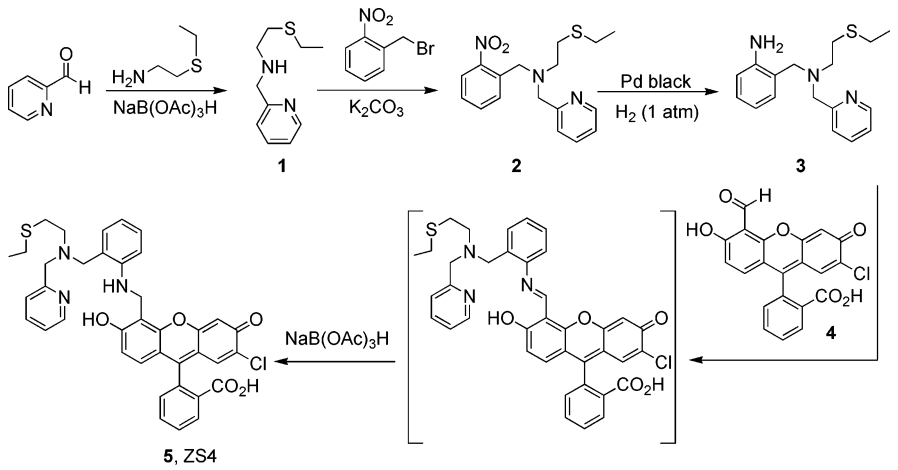

6.82 (1H, s), 7.23 (1H, d), 7.34 (1H, t), 7.50 (1H, d), 7.69−7.83 (3H, m), 8.06 (1H, d), 8.52 (1H, d). ^{13}C NMR (DMF-d_7, 125 MHz) δ 14.74, 25.45, 28.07, 48.27, 53.55, 58.83, 104.39, 110.03, 110.42, 110.57, 113.25, 117.72, 122.89, 123.91, 124.73, 125.24, 127.50, 128.01, 128.40, 130.53, 135.73, 137.29, 149.18, 150.59, 151.55, 152.31, 157.83, 158.27, 160.83, 169.08. FTIR (KBr, cm^{-1}) 3431 (m, br), 2954 (w), 2923 (w), 1760 (m), 1627 (m), 1578 (s), 1516 (m), 1489 (m), 1464 (s), 1384 (s), 1284 (m), 1259 (m), 1210 (m), 1151 (m), 1107 (m), 1091 (m), 1070 (w), 1009 (w), 871 (w), 801 (w), 759 (w), 702 (w), 622 (w), 597 (w), 551 (w), 471 (w). HRMS (ESI) Calcd MH$^+$, 575.1407. Found, 575.1428.

General Spectroscopic Procedures. Millipore water was used to prepare all aqueous solutions. A 100 mM stock solution of Zn(II) was prepared from 99.999% anhydrous $ZnCl_2$ purchased from Alrdrich. DMSO stock solutions of the ZS probes (1 mM, with the exception of 0.77 mM ZS4) were prepared, stored at −25 °C, and thawed in the dark immediately before use. A buffer containing 50 mM PIPES, piperazine-*N*,*N*′-bis(2-ethanesulfonic acid), and 100 mM KCl was used for measurements at pH 7. Data collected at pH 11 were obtained by using 50 mM CABS, 4-cyclohexylamino-1-butanesulfonic acid, 100 mM KCl as the buffer. Fluorescence spectra were obtained on a Hitachi F-3010 spectrophotometer. UV−vis spectra were recorded on a Hewlett-Packard 8453A diode array or on a Cary 1E scanning spectrophotometer. All samples were maintained at 25 °C ± 1 °C by means of a circulating water bath and were contained in 1 cm × 1 cm quartz cuvettes (3.5 mL volume, Starna). Quantum yields were determined relative to fluorescein in 0.1 N NaOH (ϕ = 0.95).[42] All spectroscopic measurements were conducted by following previously described methodology.[36,39]

Results and Discussion

Syntheses. Two general strategies for the assembly of fluorescein-based metal ion sensors have been employed in our laboratory.[36,37,39] These methodologies include the following: (i) Mannich reactions between a 2′,7′-disubstituted fluorescein and the iminium ion condensation product of paraformaldehyde and a secondary amine, which yield symmetrical sensors with two metal ion coordination sites; and (ii) stepwise routes that afford asymmetrical sensors with one metal ion binding site. The general applicability of these synthetic approaches is further illustrated in the present work.

(42) Brannon, J. H.; Madge, D. *J. Phys. Chem.* **1978**, *82*, 705−709.

The synthesis of the pyridine−amine−thioether ligand, **1**, the fragment common to all sensors in the ZS family, is shown in Scheme 1. Combination of 2-(ethylthio)ethylamine and 2-pyridinecarboxaldehyde in dry MeOH followed by reduction of the intermediate Schiff base with $NaB(OAc)_3H$ afforded **1** in moderate yield (56%) following purification on silica gel (10:1 $CHCl_3$/MeOH) as a volatile yellow-brown oil with a faint odor. We note that this reaction is concentration-dependent and adequate solvent must be used for the reaction to proceed reproducibly. Without further modification, **1** can be used in the construction of metal ion sensors that contain a tertiary amine as the PET quenching moiety (vide infra) analogous to the DPA-derived sensors ZP1−ZP3. Scheme 1 also illustrates the route to the aniline-derivatized compound **3**, which serves as the ligand fragment for ZS4 and is analogous to the DPA-incorporated metal-binding unit found in sensors ZP4−ZP8. The synthesis of **3** was accomplished in two additional steps, each of good yield. Combination of **1** with 1 equiv of 2-nitrobenzylbromide and excess K_2CO_3 in dry MeCN afforded **2** as a yellow-orange oil in 73% yield after purification on silica gel (3:1 hexanes/EtOAc). Hydrogenation of **2** in MeOH using Pd black followed by chromatography on Al_2O_3 with a solvent gradient (5:1 to 1:1 hexanes/EtOAc) gave pure **3** as a yellow-orange oil in 68% yield. Compounds **1**−**3** are stable for months when stored at 4 °C.

Sensors ZS1 and ZS2 were assembled via Mannich reactions between either 2′,7′-dichlorofluorescein (ZS1) or 2′,7′-difluorofluorescein (ZS2) and the iminium ion condensation product of **1** and paraformaldehyde, as indicated in Scheme 2. Unlike the ZP sensors, which precipitate from refluxing MeCN/H_2O mixtures, ZS1 and ZS2 remained in solution even after cooling to 0 °C. Following solvent removal, the crude sensors were purified by preparative TLC on octadecyl-functionalized silica gel (100% MeOH). ZS1 and ZS2 were both obtained as orange-red solids in moderate to good yields of 67% and 39%, respectively.

The syntheses of ZS3 and ZS4 are outlined in Schemes 1 and 2. In both cases, the chemosensors were assembled from an asymmetrical fluorescein derivatized in the 4′ position with either a benzyl bromide (ZS3) or a carboxaldehyde

Scheme 2

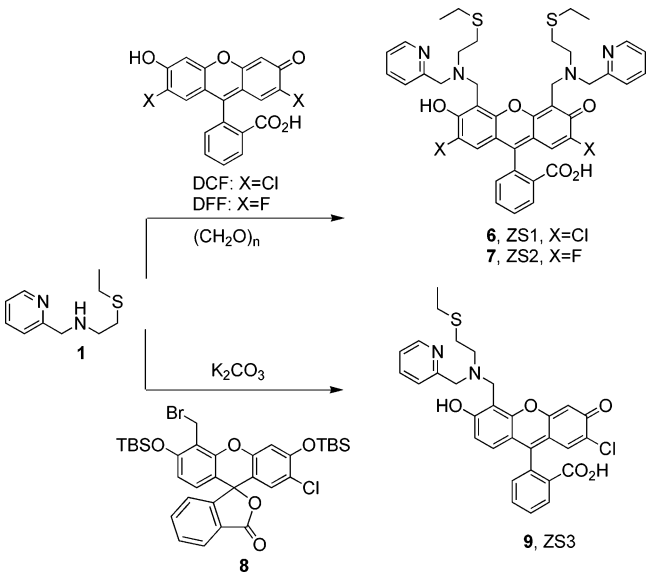

(ZS4). Combination of **1** and 1 equiv of **8** with excess K_2CO_3 in dry MeCN gave crude ZS3. The TBS protecting groups of **8** are unstable to these conditions, and deprotection occurs during the course of the reaction. Purification by preparative TLC on octadecyl-functionalized silica gel (100% MeOH) afforded ZS3 as an orange solid in 83% yield. Combination of **3** with 7′-chloro-4′-fluoresceincarboxaldehyde, **4**, in dry EtOAc resulted in precipitation of the intermediate Schiff base as a bright yellow solid. After filtration, the intermediate imine was reduced by using $NaB(OAc)_3H$ in DCE to afford crude ZS4 in 60% yield (purity ~90%). Preparative TLC on octadecyl-functionalized silica gel (100% MeOH) of a portion of the crude material yielded pure ZS4 as a red-orange solid (56% of material recovered).

Spectroscopic Characterization. Table 1 summarizes the fluorescence and optical absorption spectroscopic properties for the dyes investigated here, together with several other zinc sensors developed in our laboratory for comparison. Like the ZP probes, the ZS dyes are intensity-based sensors that utilize a tertiary amine (ZS1−ZS3) or an aniline nitrogen atom (ZS4) as the PET switch. In the absence of metal ion, the lone pair on nitrogen can donate an electron into the excited state of the fluorescein moiety, which results in fluorescence quenching. Upon alleviation of PET by addition of the appropriate cation, the fluorescein fluorescence is restored, resulting in increased emission intensity.[43,44]

Spectroscopic Properties of ZS1 and ZS2. The sensitivity of the PET-based ZP sensors to protonation is well documented.[35−40] To assess the effect of pH on the emission of free ZS1 and ZS2, fluorescence titrations were conducted. Representative data are given in Figure 2. ZS1 and ZS2 exhibit similar pH-dependent fluorescence spectral properties. Two protonation events alter the emission of apo ZS1 and ZS2, with the former exhibiting values for pK_{a1} of 7.7 and for pK_{a2} of 2.0, and for the latter, pK_{a1} is 7.7 and pK_{a2} is 2.7. In both instances, pK_{a1} is assigned to protonation of the tertiary amine responsible for PET quenching of the free probe. pK_{a2} is attributed to protonation of the fluorescein fragment and formation of a nonfluorescent isomer at low pH.[36,39] Under simulated physiological conditions (50 mM PIPES, 100 mM KCl, pH 7) and in the presence of EDTA to scavenge any adventitious metal ions, apo ZS1 and ZS2 exhibit quantum yields of 0.50 (λ_{max} = 531 nm) and 0.39 (λ_{max} = 523 nm), respectively. These data show that substitution of the chlorine atoms at the 2′ and 7′ positions of the fluorescein in ZS1 with fluorine to give ZS2 decreases the quantum yield of the unbound dye without influencing the pK_a of the tertiary amine nitrogen atom responsible for PET quenching in the apo form. These results are surprising to us, given our earlier study investigating the effect of fluorescein halogenation on the properties of ZP sensors.[38] A comparison of ZP1 and ZP3 indicated that substitution of chlorine for fluorine atoms at the 2′ and 7′ positions of the fluorescein moiety reduced the background fluorescence (ZP1, ϕ = 0.38; ZP3, ϕ = 0.15) and significantly lowered the tertiary amine pK_a (ZP1, pK_a = 8.4; ZP3, pK_a = 6.8). A comparison of the ZS1/ZS2 to the ZP1/ZP3 results reveals that the effect of fluorescein halogenation on the tertiary amine pK_a depends on the nature of the ligand. In contrast, substitution of chlorine with fluorine atoms at the 2′ and 7′ positions of the fluorescein results in decreased background fluorescence for both ligand moieties. As indicated in Table 1, the data for ZP4 and ZP8, which utilize aniline nitrogen atoms as PET switches, parallel those for ZP1 and ZP3. The comparisons between ZP and ZS sensors suggest that the magnitude of the quantum yield for an apo sensor is not solely a function of nitrogen pK_a. Theoretical calculations are in progress to investigate this matter further.

Modest fluorescence enhancement is observed upon addition of excess Zn(II) to aqueous solutions of ZS1 and ZS2. For both sensors, ϕ is ~0.7 for the Zn(II) complexes, with ZS1 displaying a ~1.4-fold increase and ZS2 a ~2-fold increase in integrated emission (Figure 3). Both emission and optical absorption spectra for free ZS1 and ZS2 are dominated by the fluorescein chromophore and blue-shift slightly upon Zn(II) coordination (Table 1). Although a ~5 nm blue-shift occurs in the emission spectra, there is a ~10 nm blue shift in the optical absorption spectra for each dye upon Zn(II) coordination. For ZS1, the absorption maximum shifts from 510 nm (ϵ = 83 900 M^{-1} cm^{-1}) to 501 nm (ϵ = 75 200 M^{-1} cm^{-1}), and the difference spectrum shows an absorption decrease at 515 nm and increases at 462 and 493 nm. ZS2 exhibits a 10 nm shift from 499 (ϵ = 66 900 M^{-1} cm^{-1}) to 489 nm (ϵ = 67 600 M^{-1} cm^{-1}), and the difference spectrum shows an absorption decrease at 506 nm and increases at 454 and 484 nm. The blue-shifts in the optical absorption spectra upon Zn(II) addition reflect a perturbation of the fluorescein π-system and may indicate the phenol oxygen atom to be involved in Zn(II) binding. Like the ZP probes, ZS1 and ZS2 display enhanced fluorescence upon the addition of Cd(II) (Table 1).

(43) de Silva, A. P.; Gunaratne, Q. N.; Gunnlaugsson, T.; Huxley, A. J. M.; McCoy, C. P.; Rademacher, J. T.; Rice, T. E. *Chem. Rev.* **1997**, *97*, 1515−1566.
(44) Czarnik, A. W. *Acc. Chem. Res.* **1994**, *27*, 302−308.

Table 1. Spectroscopic Data for ZS and Selected ZP Sensors

		absorption (λ/nm, $\epsilon/\times 10^4$ M^{-1} cm^{-1})		emission (λ/nm, Φ)[a]			
	M(II)	unbound	bound	unbound	bound	pK_a[b]	pK_a[c]
ZS1[d]	Zn	510, 8.39	501, 7.52	531, 0.50	526, 0.70	7.7	2.0
	Cd		511, 7.52		534, 0.70		
ZS2[d]	Zn	499, 6.69	489, 6.76	523, 0.39	516, 0.69	7.7	2.7
	Cd		498, 6.76		525, 0.71		
ZS3[d]	Zn	500, 8.69	ND[i]	525, 0.71	525, ND[i]	9.3	4.5
ZS3[e]	Zn	500, 7.64	503, 7.57	525, 0.07	522, 0.17		
	Cd		500, 8.37		527, 0.69		
ZS4[d]	Zn	507, 8.11	495, ND[i]	522, 0.12	520, 0.50	7.6	5.1
	Cd		498, 8.99		521, 0.50		
ZP1[d,f]	Zn	515, 6.7	507, 7.8	531, 0.38	527, 0.87	8.4	2.8
ZP3[d,f]	Zn	502, 7.5	492, 8.5	521, 0.15	516, 0.92	6.8	2.0
ZP4[d,g]	Zn	506, 6.1	495, 6.7	521, 0.06	515, 0.34	7.2	4.0
ZP8[d,h]	Zn	500, 8.1	489, 7.8	516, 0.03	510, 0.35	6.5	4.1

[a] Quantum yields relative to fluorescein in 0.1 N NaOH ($\Phi = 0.95$).[42] [b] pK_a of the amine nitrogen atom responsible for PET quenching of the unbound dye. [c] pK_a for formation of a nonfluorescent isomer. [d] Data obtained at pH 7 in 50 mM PIPES, 100 mM KCl. [e] Data obtained at pH 11 in 50 mM CABS, 100 mM KCl. [f] See refs 36 and 38. [g] See ref 37. [h] See ref 40. [i] ND = not determined.

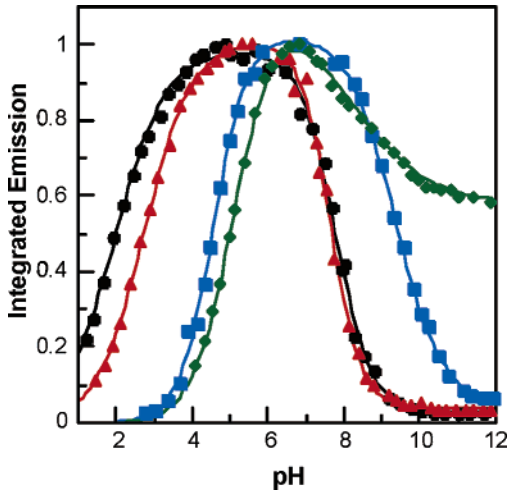

Figure 2. Fluorescence dependence on pH for ZS1−4. A 1 μM solution of each dye was prepared in 10 mM KOH, 100 mM KCl, pH ~12, and the emission spectrum collected. The pH was decreased in increments of ~0.25 by addition of 6, 2, 1, 0.5, or 0.1 N HCl, and the emission spectrum was recorded at each point. The data were integrated from 450 to 650 nm and fit according to the equation described elsewhere.[36] pK_a values are given in Table 1. Black circles: ZS1, λ_{ex} = 510 nm; red triangles, ZS2, λ_{ex} = 499 nm; blue squares, ZS3, λ_{ex} = 500 nm; green diamonds, ZS4, λ_{ex} = 504 nm.

Spectroscopic Properties of ZS3. Fluorescence spectroscopy was used to monitor the pH dependent properties of ZS3, revealing two protonation events that alter ZS3 fluorescence with pK_{a1} = 9.3 and pK_{a2} = 4.5 (Figure 2). The former value is assigned to protonation of the tertiary amine atom responsible for PET quenching of the unbound dye and the latter to protonation of the fluorescein and formation of a nonfluorescent species.[36,39] ZS3 maintains its maximum fluorescence from pH ~6 to pH ~8, and the relatively high value of pK_{a1} suggests that protonation of the tertiary amine will interfere with PET quenching of the fluorescein moiety at neutral pH (Figure 3). In accord with this notion, free ZS3 exhibits a quantum yield of 0.71 (λ_{max} = 525 nm) at pH 7 and in the presence of EDTA to complex any potentially interfering metal ions. The absorption spectrum of ZS3 has a maximum at 500 nm (ϵ = 86 900 M^{-1} cm^{-1}). As a result of the high quantum yield of apo ZS3, essentially no fluorescence increase occurs upon addition of excess Zn(II) to ZS3 at neutral pH. We note that addition of excess Cd(II) causes a ~10% fluorescence increase and excess Hg(II) causes a ~40% fluorescence decrease at pH 7.

The high background fluorescence of ZS3 renders it unsuitable for any sensing applications at neutral pH. To investigate further PET and the effect of the pyridyl/thioether ligand substitution, we conducted several studies at pH 11, which should favor deprotonation of the tertiary amine atom and decrease background fluorescence. At pH 11 (50 mM CABS, 100 mM KCl), the fluorescence of unbound ZS3 is effectively quenched, giving rise to a quantum yield of 0.07 (λ_{max} = 525 nm), and a ~2.4-fold fluorescence enhancement occurs upon addition of excess Zn(II) (ϕ = 0.17). The molar absorptivity of the free dye is also diminished at pH 11 (ϵ_{500} = 76 400 M^{-1} cm^{-1}) and shows negligible change upon Zn(II) addition (ϵ_{503} = 75 700 M^{-1} cm^{-1}). Coordination of ZS3 to Cd(II) and Hg(II) yields a relatively greater fluorescence enhancement at pH 11 than that observed for Zn(II). Upon addition of excess Cd(II) to CS1 at pH 11, a ~15-fold increase in integrated emission is observed (λ_{max} = 527 nm, ϕ = 0.69; ϵ_{500} = 83 700 M^{-1} cm^{-1}), and excess Hg(II) causes a ~5.7-fold fluorescence enhancement (λ_{max} = 530 nm, ϕ = 0.40; ϵ_{505} = 84 100 M^{-1} cm^{-1}). Job plots and metal ion binding titrations conducted at pH 11 indicate that ZS3 forms a 1:1 complex with all three group 12 metal ions (Figures S1 and S2, Supporting Information.)

Spectroscopic Properties of ZS4. Sensor ZS4 contains an aniline-derivatized (2-ethylsulfanylethyl)pyridin-2-yl-methylamine moiety (Scheme 1). On the basis of previous studies in our laboratory comparing ZP1 to ZP3 with ZP4 to ZP8, we anticipated that ZS4 would exhibit lower background fluorescence than ZS1−ZS3. As expected, at pH 7 and 100 mM ionic strength, free ZS4 has a quantum yield of 0.12 (λ_{max} = 522 nm) compared to 0.71 for ZS3, 0.50 for ZS1, and 0.39 for ZS2. The fluorescence pH profile of ZS4, depicted in Figure 1, shows two changes deriving from pK_{a1} = 7.6 and pK_{a2} = 5.1. The former, assigned to the aniline nitrogen atom, indicates that the nitrogen lone-pair is

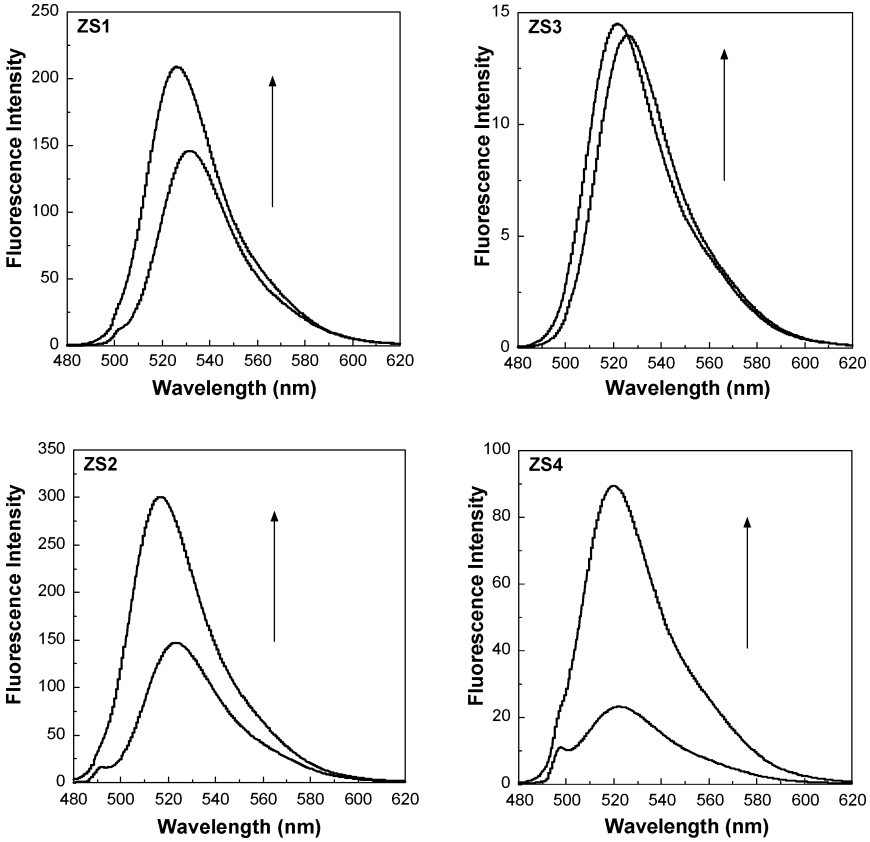

Figure 3. Fluorescence spectra of ZS probes before and after the addition of 67 equiv of Zn(II) at pH 7 (50 mM PIPES, 100 mM KCl). All probe concentrations are 1 μM. Excitation and emission slits were set at 3 nm with the exception of the ZS3 measurements, where 1.5 nm slits were used. Upper left: ZS1, $\lambda_{ex} = 500$ nm. Lower left: ZS2, $\lambda_{ex} = 489$ nm. Upper right: ZS3, $\lambda_{ex} = 500$ nm. Lower right: ZS4, $\lambda_{ex} = 495$ nm.

available for PET quenching at neutral pH, and the latter is assigned to formation of a nonfluorescent isomer. As indicated in Figure 3, sensor ZS4 exhibits a ~4.5-fold fluorescence enhancement immediately after addition of excess Zn(II) and a quantum yield of 0.50 ($\lambda_{max} = 520$ nm) at neutral pH. A ~25% decrease in fluorescence intensity is observed several minutes after mixing of the ZS4/Zn(II) solution, which contrasts with the stable fluorescence increase observed for ZP and other ZS species upon Zn(II) addition. Unexpected changes were also observed in the optical absorption spectra (Figure 4). Upon introduction of Zn(II) to a solution of ZS4, the absorption spectrum initially undergoes a blue-shift from 507 ($\epsilon = 81\ 100\ M^{-1}\ cm^{-1}$) to 495 nm (spectra a and b). Over the course of ~15 min, A_{max} decreases substantially, and a shoulder develops at ~530 nm (spectra b and c). Inspection of the sample revealed formation of a precipitate, supported by the rising baseline in the red region of the optical spectrum, arising from light scattering. Upon introduction of excess EDTA, the absorption spectrum undergoes a red-shift back to 507 nm with no change in A_{max} immediately after mixing (spectra c and d). Over the course of several hours, the absorption spectrum for the EDTA-containing solution becomes comparable to the initial spectrum of free ZS4 (spectra d and e). These data indicate that ligand decomposition is not responsible for the spectral changes observed upon introduction of Zn(II) to a solution of ZS4.

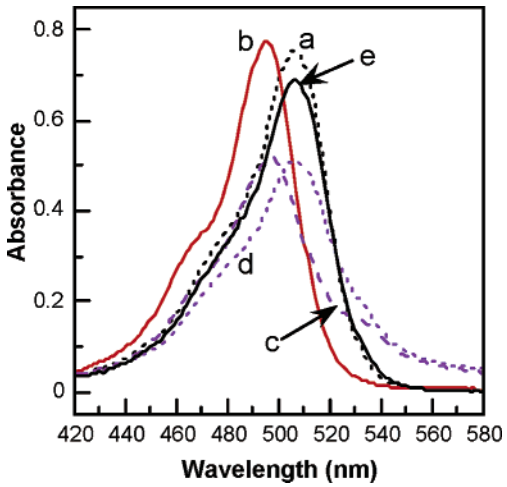

Figure 4. Optical absorption spectra for ZS4 in 50 mM PIPES, 100 mM KCl, pH 7. Black dotted line (a): ZS4, 10 μM. Red solid line (b): spectrum immediately after addition of 10 equiv Zn(II) to a. Purple dashed line (c): solution b after ~15 min. Purple dotted line (d): addition of 100 equiv EDTA to c. Black solid line (e): the change in spectrum d after several hours. Precipitation was observed several minutes after addition of Zn(II), and the precipitate was no longer apparent after addition of EDTA.

Under identical conditions, stable fluorescence enhancement of ZS4 is observed upon introduction of Cd(II) or Hg(II), although the increase upon Hg(II) addition is negligible. The presence of excess Cd(II) causes a ~4-fold fluorescence increase in integrated emission ($\lambda_{max} = 521$ nm, $\phi = 0.50$), and the absorption spectrum blue-shifts to 498

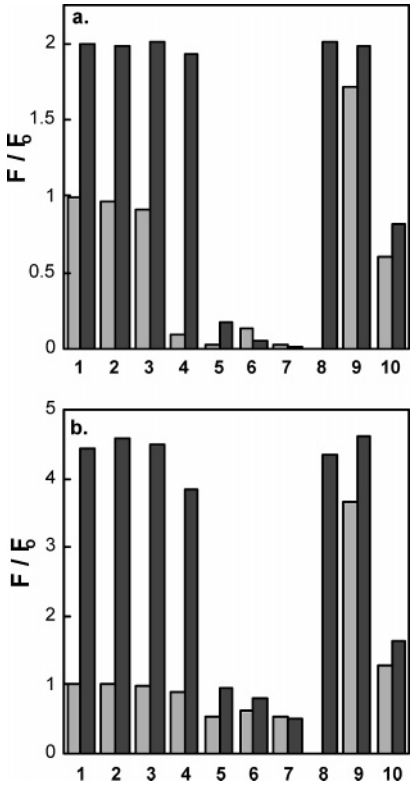

Figure 5. Selectivity of representative ZS probes for Zn(II) over other metal ions under simulated physiological conditions (50 mM PIPES, 100 mM KCl, pH 7). The light gray bars represent the emission of the ZS probe in the presence of 67 equiv of the cation of interest: 1, Ca(II); 2, Mg(II); 3, Mn(II); 4, Fe(II); 5, Co(II); 6, Ni(II); 7, Cu(II); 8, Zn(II); 9, Cd(II); 10, Hg(II). The dark gray bars represent the fluorescence change that occurs when 67 equiv of Zn(II) is added to each solution. The response (F) is normalized with respect to free ZS (F_o). (a) ZS2 response and excitation was provided at 500 nm. The data were integrated from 450 to 650 nm. (b) ZS4 response and excitation was provided at 495 nm. The data were integrated from 510 to 650 nm.

nm (ϵ = 89 900 M^{-1} cm^{-1}). Job plots for the addition of Cd(II), Hg(II), and Cu(II) to solutions of ZS4 indicate formation of well-defined 1:1 complexes (Figure S3, Supporting Information). Given the water solubility of these 1:1 complexes and that the Zn(II) complexes of MS1 and ZP4 do not precipitate from aqueous solution, the insolubility of the ZS4:Zn(II) complex was a surprise. Although we speculate that the ZS4:Zn(II) species may be some dimeric or polymeric species, its exact nature is currently unknown.

Metal Ion Selectivity. Achieving Zn(II) selectivity over other divalent first-row transition metal ions while maintaining adequate fluorescence turn-on upon coordination is an important goal and the main focus of this investigation. As stated above, we anticipated that replacement of one pyridyl arm of a ZP sensor with a soft sulfur donor, such as the thioether moiety utilized in this work, might improve selectivity for Zn(II). All ZS sensors exhibit analogous metal ion selectivity, and Figure 5 illustrates the results of these studies for representative sensors ZS2 and ZS4. Both molecules are selective for Zn(II) over Ca(II), Mg(II), Mn(II), and Fe(II). The selectivity for Zn(II) over Fe(II) is a significant advantage over the behavior observed for DPA-derived zinc sensors.

Summary

The syntheses of four water-soluble, fluorescein-based Zn(II) sensors of the Zinspy family, which contain one or two pyridyl−amine−thioether ligands, are described. The assembly of these compounds illustrates the generality of the synthetic approach originally designed to create symmetric and asymmetric ZP sensors. Whereas ZS1, ZS2, and ZS4 display ∼1.4- to ∼4.5-fold fluorescence enhancement upon Zn(II) complexation under simulated physiological conditions, the high background fluorescence of ZS3 allows only negligible fluorescence turn-on upon addition of Zn(II) at neutral pH. Due to the presence of a soft thioether donor in the coordination sphere, the ZS sensors exhibit improved selectivity for Zn(II) over the DPA-based ZP sensors. Comparisons of the photophysical properties of symmetric ZS1/ZS2 and ZP1/ZP3 couples provide further insight into the effect(s) of the ligand, fluorescein halogenation, and tertiary amine pK_a on PET quenching of unbound xanthene-substituted fluorescein-based dyes. Systematic studies such as this one are necessary to reveal the features required for the further improvement of sensors to understand the roles of zinc in neurobiology.

Acknowledgment. This work was supported by Grant GM65519 from the Institute of General Medical Sciences. Spectroscopic instrumentation at the MIT DCIF is maintained with funding from NIH Grant 1S10RR13886-01 and NSF Grants CH3-9808063, DBI9729592, and CHE-9808061. E.M.N. thanks NDSEG for a graduate fellowship.

Supporting Information Available: Figures S1, S2, and S3 showing Job plots and metal binding titrations for sensors ZS3 and ZS4 with various divalent metal ions. This material is available free of charge via the Internet at http://pubs.acs.org.

IC048778Z